METEORITICS & PLANETARY SCIENCE

Table of Contents

Volume 37 Number 9 2002 September

Articles

A. JAMBON, J. A. BARRAT, V. SAUTTER, PH. GILLET, C. GÖPEL, M. JAVOY, J. L. JORON AND M. LESOURD: The basaltic shergottite Northwest Africa 856: Petrology and chemistry 1147

The Mercury 2001 workshop

A. E. POTTER, R. M. KILLEN AND T. H. MORGAN: The sodium tail of Mercury 1165

P. L. KOEHN, T. H. ZURBUCHEN, G. GLOECKLER, R. A. LUNDGREN AND L. A. FISK: Measuring the plasma environment at Mercury: The fast imaging plasma spectrometer 1173

D. M. HUNTEN AND A. L. SPRAGUE: Diurnal variation of sodium and potassium at Mercury 1191

L. V. POTTS, R. R. B. VON FRESE AND C. K. SHUM: Crustal properties of Mercury by morphometric analysis of multi-ring basins on the Moon and Mars 1197

S. M. MILKOVICH, J. W. HEAD AND L. WILSON: Identification of mercurian volcanism: Resolution effects and implications for MESSENGER 1209

R. M. KILLEN: Source and maintenance of the argon atmospheres of Mercury and the Moon 1223

T. H. BURBINE, T. J. MCCOY, L. R. NITTLER, G. K. BENEDIX, E. A. CLOUTIS AND T. L. DICKINSON: Spectra of extremely reduced assemblages: Implications for Mercury 1233

D. T. BLEWETT, B. R. HAWKE AND P. G. LUCEY: Lunar pure anorthosite as a spectral analog for Mercury 1245

A. L. SPRAGUE, J. P. EMERY, K. L. DONALDSON, R. W. RUSSELL, D. K. LYNCH AND A. L. MAZUK: Mercury: Mid-infrared (3–13.5 μm) observations show heterogeneous composition, presence of intermediate and basic soil types, and pyroxene 1255

S. J. PEALE, R. J. PHILLIPS, S. C. SOLOMON, D. E. SMITH AND M. T. ZUBER: A procedure for determining the nature of Mercury's core 1269

Cover: In this issue we publish a series of papers on Mercury from a workshop entitled "Mercury: Space Environment, Surface and Interior" that was held at the Field Museum in Chicago, Illinois on 2001 October 4–5. The cover of this issue sets the mood for the series. *(Top)* Mercury is the least explored of the terrestrial planets. Despite its lunar-like surface, from bulk density alone we know that it has a very different composition from that of the Moon or any of the terrestrial planets. Our knowledge of Mercury is nonetheless very limited, and we are still debating fundamental questions. Has Mercury experienced surface volcanism? At what solar distance was Mercury formed? Is Mercury's magnetic field the result of a core dynamo? *(Lower left)* An unusual group of chondrites containing up to 80% metal coexisting with very-low-FeO silicates may be similar in bulk composition to Mercury. In this reflected light photograph of the Weatherford meteorite, metal grains are bright and silicate is dark (photo courtesy of Sasha Krot, Smithsonian Institution). *(Lower right)* The impact that formed Mercury's Caloris basin (1340 km diameter) excavated deep into the crust and possibly even the upper mantle (Mariner 10 mosaic; latitude and longitude are shown at 10° increments). This region may provide our best chance to infer Mercury's upper mantle composition and thus estimate the composition of the bulk silicate portion of the planet (Mariner 10 mosaics courtesy of Mark Robinson, Northwestern University). *(Overlay)* These questions and many others will be addressed with a suite of scientific instruments aboard NASA's MESSENGER (MErcury Surface, Space ENvironment, GEochemistry, and Ranging) spacecraft scheduled to be launched in 2004 and to orbit Mercury for one Earth year beginning in 2009. The MESSENGER mission, led by Principal Investigator Sean C. Solomon of the Carnegie Institution of Washington, is being built and operated by The Johns Hopkins University Applied Physics Laboratory.

ELECTRONIC SERVICES
http://www.uark.edu/meteor

ScienceMAPS: Readers can have the Table of Contents for upcoming issues of the journal sent directly to their e-mail account as soon as each issue is closed. Requests may be made at the journal website.

Abstracts of articles to appear in the next issue may be previewed at the journal website four to eight weeks before publication. Abstracts are posted within a few days of formal acceptance by the Editor. ***Contents pages*** for the next issue may also be viewed. Information for contributors and order forms are available also.

For subscribers only:

Prelude: A preprint service of *Meteoritics & Planetary Science*. Every article accepted for publication is placed on the journal website at a secure location within days of formal acceptance by the editor. Thus, articles are published as electronic preprints, in the author's format, two to three months earlier than they will appear in the hard copy and electronic journal.

Electronic edition of MAPS: Current volumes of *Meteoritics & Planetary Science* are available electronically at a secure location on the journal's website. Older volumes are available electronically at the Astrophysical Data Service website.

Meteoritics & Planetary Science is indexed in *Chemical Abstracts, Current Contributions, INSPEC, ASCA, Deep Sea Research & Oceanography Abstracts, Georef., International Aerospace Abstracts, Indiana Science Reviews, Geological Abstracts, Mineralogical Abstracts, Science Citation Index* and is posted at the Astrophysical Data Service website, which is fully searchable, twelve months after hard copy publication.

Editorship of *Meteoritics and Planetary Science*

Dr. A. J. T. Jull of the University of Arizona will become the editor of *Meteoritics and Planetary Science* on January 1, 2003.

New manuscripts received after September 1, 2002 will be forwarded to the incoming editor, Dr. Jull.

Manuscripts currently in review or revision will continue to be handled at the Arkansas office until December 15, 2002 at which point they will be forwarded to the incoming editor.

Forward

Return to Issues Listing

Meteoritics & Planetary Science 37, 1147–1164 (2002)
Available online at http://www.uark.edu/meteor

The basaltic shergottite Northwest Africa 856: Petrology and chemistry

A. JAMBON[1]*, J. A. BARRAT[2], V. SAUTTER[3], PH. GILLET[4], C. GÖPEL[5], M. JAVOY[6], J. L. JORON[7] AND M. LESOURD[8]

[1]Laboratoire Magie, Université Pierre et Marie Curie, IPGP, CNRS UMR 7047, case 110, 4 place Jussieu, 75252 Paris cedex 05, France
[2]CNRS UMR 6112 (Géodynamique et Planétologie) and Université d'Angers, 2 bd Lavoisier, 49045 Angers cedex, France
[3]Laboratoire de Minéralogie, Muséum National d'Histoire Naturelle, 61 rue Buffon, 75005 Paris, France
[4]Laboratoire des Sciences de la Terre, CNRS UMR 5570, Ecole Normale Supérieure de Lyon, 46 Allée d'Italie, 69364 Lyon Cedex 7, France
[5]Laboratoire de Géochimie et Cosmochimie, Institut de Physique du Globe de Paris, CNRS UMR 7579, 4 place jussieu, 75252 Paris cedex 05, France
[6]Laboratoire de Géochimie des Isotopes stables, Institut de Physique du Globe de Paris, CNRS UMR 7047, 4 place jussieu, 75252 Paris cedex 05, France
[7]Groupe des Sciences de la Terre, laboratoire Pierre Süe, CE saclay, 91191 Gif sur Yvette cedex, France
[8]SCIAM, Laboratoire d'Histologie, UFR de Médecine, Université d'Angers, 1 rue Haute de Reculée, 49045 Angers cedex, France
*Correspondence author's e-mail address: jambon@ccr.jussieu.fr

(Received 2001 December 18; accepted in revised form 2002 May 21)

Abstract–We report on the discovery of a new shergottite from South Morocco. This single stone weighing 320 g is referenced as Northwest Africa (NWA) 856 with Djel Ibone as a synonymous name. It is a fresh, fine-grained basaltic rock consisting mainly of two pyroxenes (total ~68 vol%: 45% pigeonite, $En_{61–16}Wo_{9–22}Fs_{26–68}$; 23% augite, $En_{46–26}Wo_{34–29}Fs_{21–43}$) and plagioclase converted to maskelynite (~23 vol%, $Ab_{43–57}Or_{1–5}An_{54–36}$). Accessory minerals include merrillite, Cl-apatite, pyrrhotite, ilmenite, ulvöspinel, silica (stishovite and glass), amorphous K-feldspar and baddeleyite. Amorphous mixtures of maskelynite and silica occur most commonly as median layers inside maskelynite laths. In addition, melt pockets (~2 vol%) were recognized with relics of maskelynite, pyroxene and both dense silica glass and stishovite occurring as both grains and submicrometer needles. The compositions of the melt pockets are consistent with mixtures of maskelynite and pyroxenes with an average of ~50 vol% maskelynite. The meteorite is highly fractured at all scales.

The bulk composition of NWA 856 has been measured for 44 elements. It is an Al-poor ferroan basaltic rock which strongly resembles Shergotty and Zagami in its major and trace element composition.

The nearly flat rare earth element (REE) pattern $(La/Lu)_n = 0.9$, is similar to that of Shergotty or Zagami and differs significantly from NWA 480, another Moroccan shergottite recently described. According to the U, Ba and Sr abundances, NWA 856 is not significantly weathered. The oxygen isotopes ($\delta^{18}O = +5.03‰$, $\delta^{17}O = +3.09‰$, and $\Delta^{17}O = +0.47‰$) are in agreement with the martian origin of this meteorite.

On the basis of grain size, pyroxene zoning and composition, abundance of silica inclusions associated with maskelynite, trace element abundances, REE pattern and oxygen isotopes, pairing with NWA 480 is excluded. The similarity with Shergotty and Zagami is striking. The only significant differences are a larger grain size, a greater abundance of silica and melt pockets, a slightly more restricted range of pyroxene compositions and the absence of significant mesostasis.

INTRODUCTION

After the first discovery of martian meteorites a second stage of discoveries occurred in Antarctica (with the recognition of their martian origin). A third stage has been ongoing for several years now, with the new finds in hot deserts: Dar al Gani (DaG) 476/489/670/735, Sayh al Uhaymir (SaU) 05/08/51/94, Dhofar (Dho) 019, Northwest Africa (NWA) 480 and 817. Theses new discoveries present an opportunity to improve our knowledge of martian meteorites: shergottites appear to form a prominent group (thirteen specimens) while nakhlites (four specimens) remain rare stones; Allan Hills (ALH) 84001 and Chassigny remain unique. Shergottites according to their mineralogy can be divided into basaltic shergottites (eight specimens if we include Elephant Moraine (EETA)79001B and NWA 856, the last discovery), picritic shergottites (five

Prelude preprint MS#4714

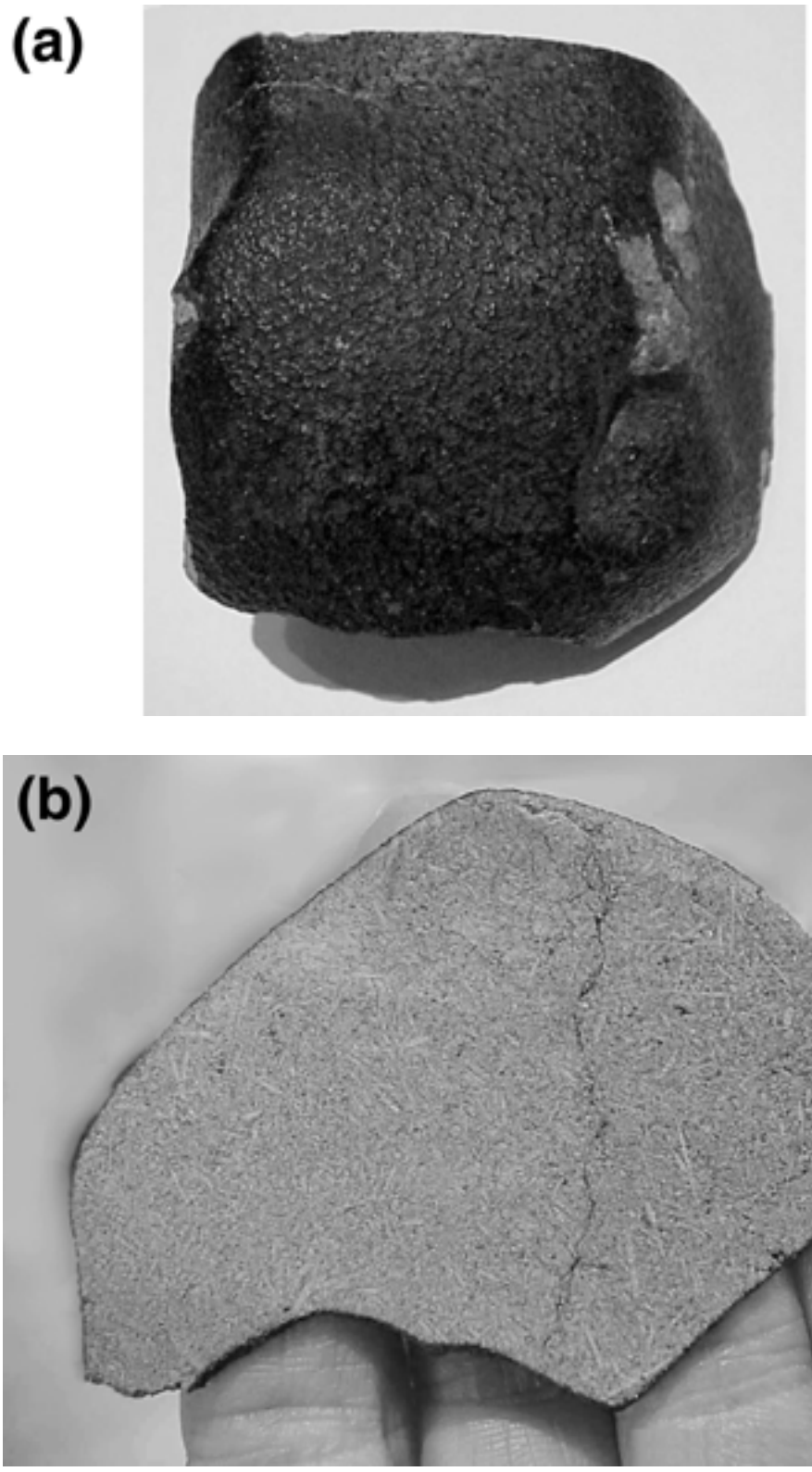

FIG. 1. (a) The mass of NWA 856 showing a well-preserved fusion crust and minor alteration. The size is ~5 cm. (b) Sawn surface of NWA 856 showing the long pyroxene needles (several millimeters). (Photographs courtesy of B. Fectay and C. Bidant of La Mémoire de la Terre.)

specimens including EETA79001A and NWA 1068) and peridotitic shergottites (three specimens).

We report on NWA 856, or Djel Ibone, the third martian meteorite from Morocco. It is a single stone of 320 g with a nearly complete, fresh fusion crust (Fig. 1a). It was found in April of 2001 by meteorite dealers in the south of Morocco and the exact location of its discovery has not been revealed.

On a sawn surface (Fig. 1b), its appearance is dominated by light green elongated pyroxenes (to a few millimeters), interstitial maskelynite, and rare opaque oxides. It will be shown that its mineralogical and geochemical properties rule out pairing with any of the previous Moroccan finds.

ANALYTICAL METHODS

Petrographic observations and quantitative chemical analyses of the various phases were made on a polished section of NWA 856 of ~0.95 cm^2. The procedures are very similar to those used for the shergottite NWA 480 (Barrat *et al.*, 2002) and nakhlite NWA 817 (Sautter *et al.*, 2002). Backscattered electron images were taken with a JEOL JSM6301-F scanning electron microscope (SEM) with an energy dispersive spectrometer (EDS) at SCIAM, Angers. Additional SEM work was performed in Paris (UPMC) with a JEOL 840-A, mostly to provide working backscattered electron images and x-ray mapping to evaluate the abundance of and locate minor phases. Electron microprobe (EMP) analyses were performed in Paris (UPMC) with a Cameca SX50 wavelength dispersive spectrometer (WDS). Operating conditions were 15 kV accelerating voltage with a probe current of 12 nA and a spot size of ~1 μm for all phases except for maskelynite and impact melts. For the latter, we used a defocused beam of 10 μm in diameter and a probe current of 8 nA as suggested by Mikouchi *et al.* (1999), in order to minimize volatile loss.

A 500 mg fragment was finely ground using a sapphire mortar and pestle. A split (120 mg) was used to determined the major and trace element abundances in Grenoble, by inductively coupled plasma-atomic emission spectrometry (ICP-AES) and inductively coupled plasma-mass spectrometry (ICP-MS), respectively. Another split of the same powder (80 mg) was used for the determination of additional trace element abundances (As, Br, Sb, Au and Ag) by instrumental neutron activation analysis (INAA) at Laboratoire Pierre Süe, Saclay. Our procedures are the same as those described by Barrat *et al.* (2000) and Joron *et al.* (1997). The accuracy on major and trace element concentrations is better than 5% in most cases, except for As (15%), and Au (30%).

The modal composition has been estimated from points counted on backscattered electron images, Ca and Mg images, and from a mass balance calculation for the phases and bulk-rock composition.

The mineralogy of the silica has been determined by Raman spectroscopy. Raman spectra were recorded on the polished section with a Dilor® XY spectrometer equipped with confocal optics and a nitrogen-cooled charge coupled-device (CCD) detector at ENS Lyon. A microscope is used to focus the excitation laser beam (488 and 514 nm lines of a Spectra Physics® Ar^+ laser) to a 2 μm spot and to collect the Raman signal in the backscattered direction. Accumulations lasted from 120 to 300 s. The laser power was restricted from 2 to 50 mW to avoid deterioration of the sample.

Oxygen isotopes were determined by laser fluorination at IPGP. A subsample of ~1 mg is reacted at a pressure of 100 mbar BrF_5 under the spot of a CO_2 Melles Griot laser (20 W). The resulting O_2 is purified over a KBr furnace and analyzed as O_2 in a VG Optima dual inlet mass spectrometer. Quartz and basalt glass standards are routinely analyzed for calibration of the system. The overall reproducibility is estimated at $\pm 0.1‰$.

RESULTS AND DISCUSSION

Petrography

This stone is nearly totally covered with glassy black fusion crust (Fig. 1). It is fresh and weathering products (such as carbonates) are limited to a few spots on the fusion crust and a few large cracks within the sample. On the sawn surface, the interior appears fine-grained crystalline and consists mainly of gray acicular pyroxene phenocrysts (the largest grains are up to 12 mm in length) and plagioclase laths converted to maskelynite of <500 μm. At smaller scale, on the backscattered electron view of the whole section, only smaller pyroxenes are recognized because of stereological considerations (Fig. 2) and because of fracturing. Maskelynite laths are commonly stacked up and interstitial to the pyroxene phenocrysts (Fig. 3). Pyroxenes rarely include oxides (*e.g.*, chromite), unlike NWA 480. Augite and pigeonite form separate crystals (as in Shergotty and Zagami) and not as complexly zoned grains as in NWA 480 and Queen Alexandra Range (QUE) 94201 (McSween *et al.*, 1996; Mikouchi *et al.*, 1999; Barrat *et al.*, 2002). In some areas, augite crystals are surrounded with a corona of pigeonite crystals and/or pigeonite and maskelynite laths. No preferred orientation of the pyroxenes was observed. Maskelynite is less abundant and is interstitial to pyroxenes and appears sometimes injected between broken pyroxenes. The maskelynite contains numerous inclusions of Fe-Ti oxides (of a few micrometers). Typically phosphates and small crystals of Fe-Ti oxides (~10 μm) are interstitial at the boundary between pyroxene and maskelynite.

Four different occurrences of silica are observed:

• Most commonly as thin patches (~20 μm) included in the middle of maskelynite laths associated with Fe-Ti oxide inclusions. Similar silica lamellae are present (although uncommon) in Zagami and are nearly absent in Shergotty and NWA 480.

• Rarely as small inclusions in ulvöspinel, surrounded by radiating cracks.

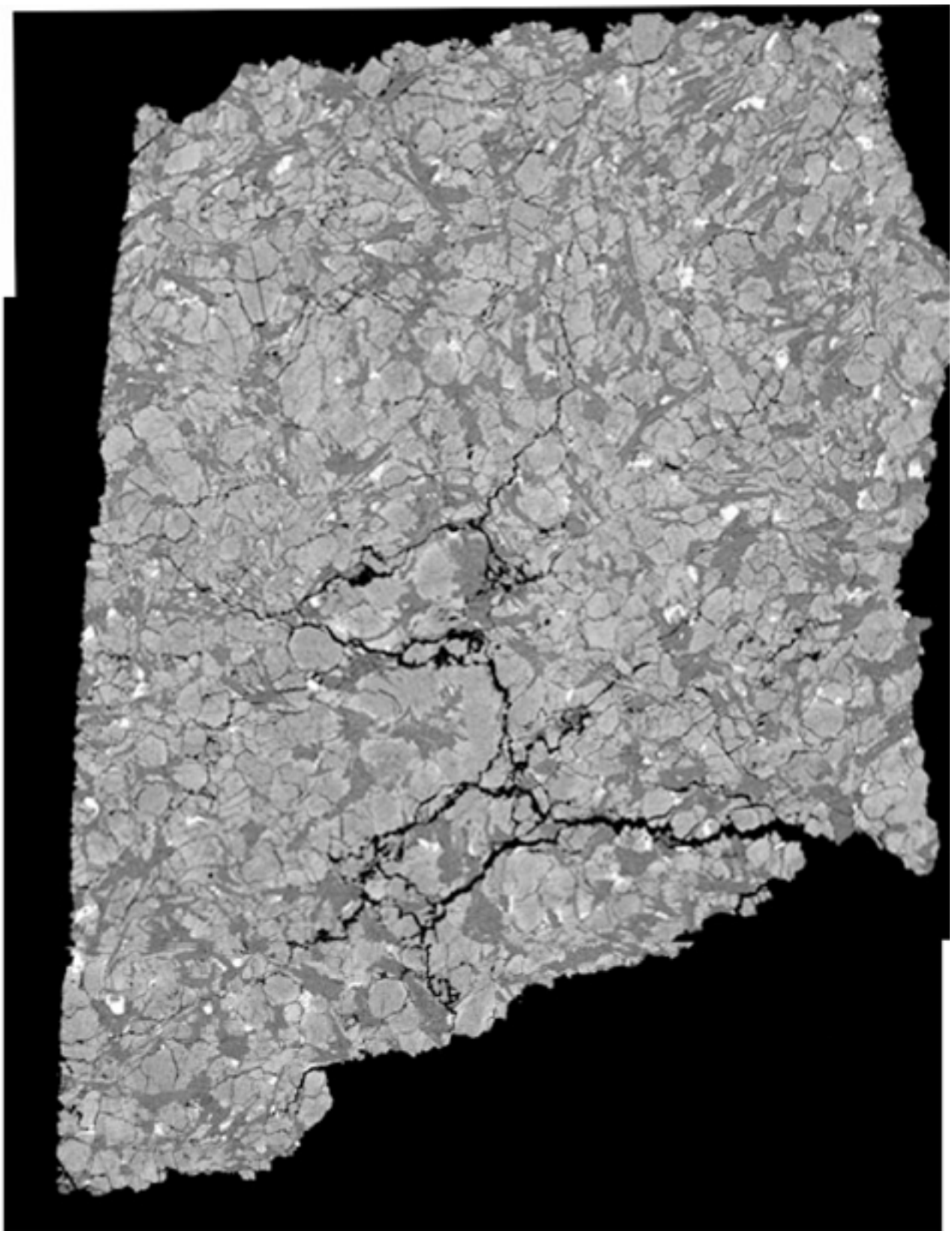

FIG. 2. Backscattered electron image of the whole polished section of NWA 856 showing dominant pyroxene (light gray), maskelynite (dark gray), and oxides (white). Notice that the apparent size of pyroxene is significantly smaller compared to those of Fig. 1b. Width of view is ~1 cm.

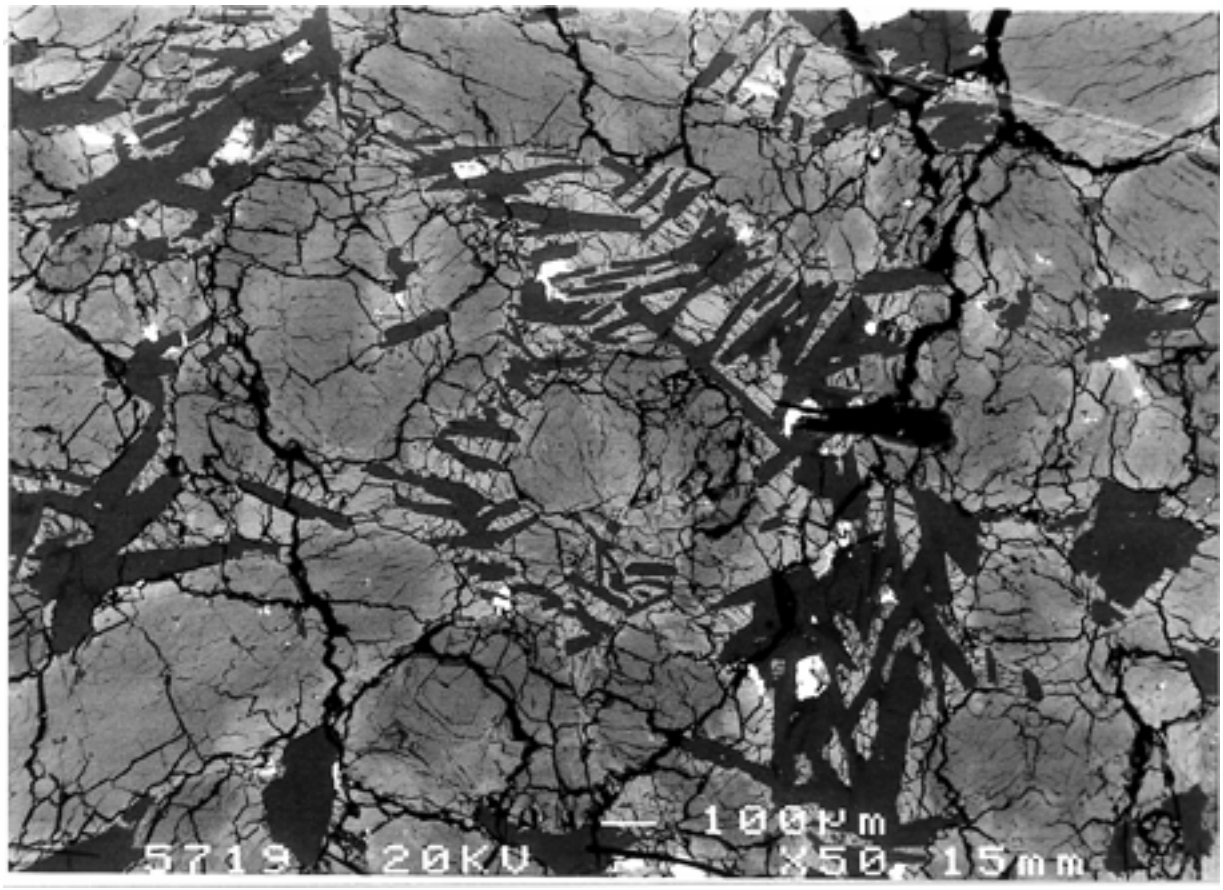

FIG. 3. Backscattered electron image (middle left of the section in Fig. 2) showing the characteristic features. Large grey crystals are zoned pyroxenes, the dark phase is maskelynite. Fe-Ti oxides, minor pyrrhotite and chromite (all white) are included in maskelynite or interstitial between maskelynite and pyroxene. Silica and silica-maskelynite glass (black) inside the maskelynite stacks. Notice the fracturation of pyroxene. Width of view is 1.5 mm.

• As wedges between maskelynite laths or between maskelynite and pyroxene, the most common texture for silica in shergottites. These silica grains resemble those recently described in Shergotty by Sharp *et al.* (1999).

• As crystals and patches in impact melt pockets (Fig. 4). It is observed as either euhedral crystals up to 200 μm, rounded patches (up to 100 μm) or very thin needles of ~1 μm with a square cross section. These needles have been identified as stishovite by Raman spectroscopy.

These occurrences are quite similar though more abundant than those already found in NWA 480 (Barrat *et al.*, 2002). Raman spectroscopy measurements show that these silica grains represent a mixture of dense silica glass and stishovite (Fig. 5). This is the third unambiguous determination of stishovite in a shergottite after Shergotty (Stöffler *et al.*, 1986; Sharp *et al.*, 1999) and NWA 480 (Barrat *et al.*, 2002). In NWA 856 melt pockets are more frequent and of larger size (of the order of a millimeter) compared to Shergotty, Zagami, Los Angeles and NWA 480.

Mode–Excluding the melt pockets, modal analyses gives the following mineral proportions: 68 vol% pyroxenes (23% augite, 45% pigeonite), 23% maskelynite, 1% phosphates (merrillite and minor chlorapatite), 2% opaque oxides (mainly ilmenite and ulvöspinel and minor chromite), rare sulfides (pyrrhotite, <0.1%), 1% silica including stishovite) and amorphous mixtures of silica and maskelynite. This modal composition is very similar to that reported for Shergotty by Hale *et al.* (1999), with the same abundance ratio of pigeonite to augite (~2).

Shock Features–The rock is extensively fractured, even more so than the other basaltic shergottites. A few large fractures cut the fusion crust and have been cemented by carbonate (a common feature of desert alteration). Pyroxene grains are highly fractured, with an increase from core to rim where numerous small fractures are observed. Commonly, the cores of pyroxenes are delimited by a circular fracture. Maskelynite, as in other shergottites, is almost devoid of fractures.

Shock melt pockets (Fig. 4) are more abundant in NWA 856 than in Shergotty, Zagami or NWA 480 (McCoy *et al.*, 1992; Marti *et al.*, 1995; Barrat *et al.*, 2002). No obvious relation appears between fractures and melt pockets. Finally

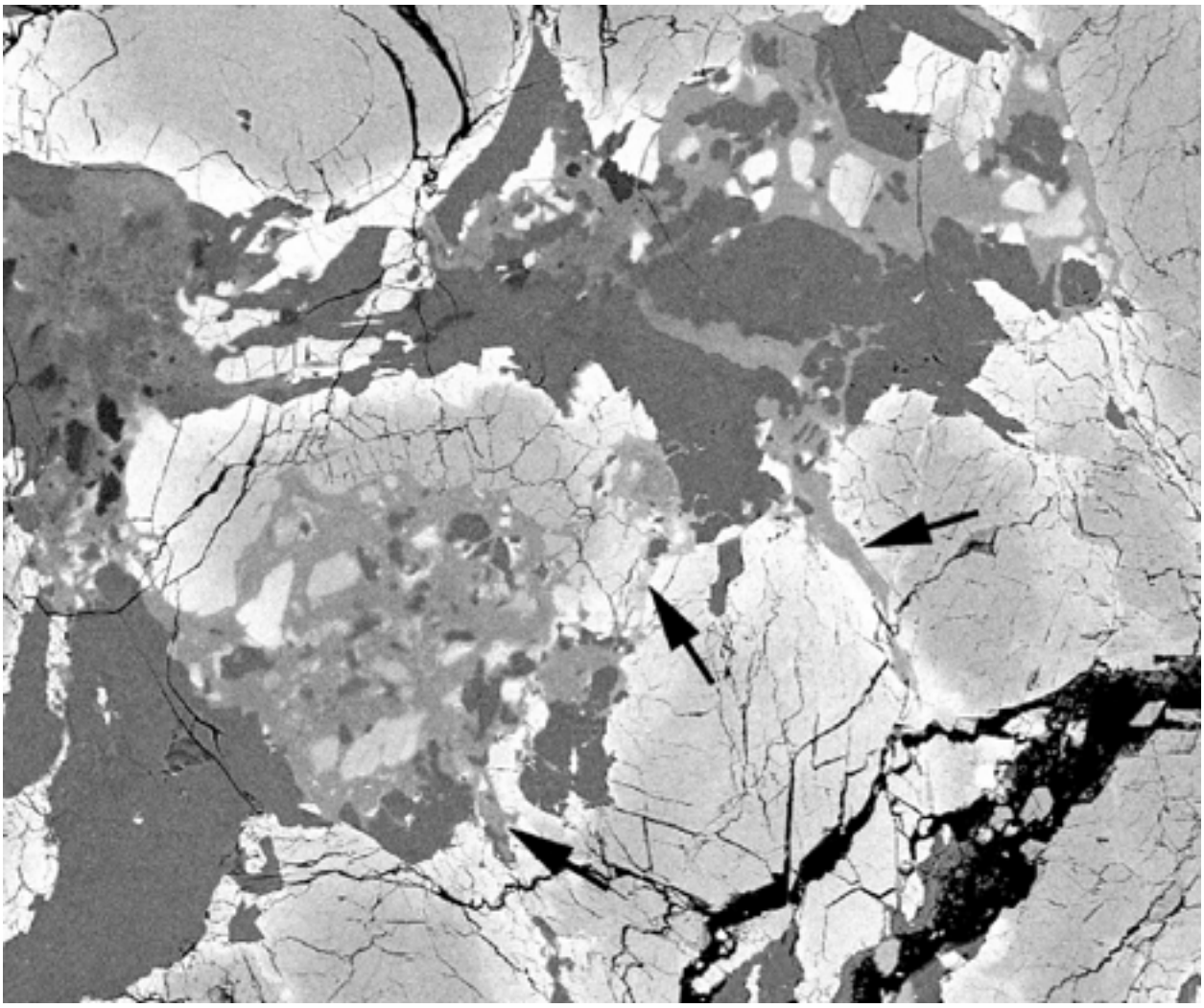

FIG. 4. Backscattered electron image of typical impact melt pockets. Residual pyroxene and maskelynite appear as rounded patches surrounded by impact glass of intermediate composition. A few dark clots correspond to silica (glass and stishovite which cannot be distinguished at this magnification). Notice that very few fractures crosscut the impact melt pockets, even less than the nearly fracture-free maskelynite. Notice that some of the melt penetrates into the pyroxene fractures (arrows) and that melt pockets are located preferentially at the boundary between pyroxene and maskelynite. Width of view is 1.5 mm.

the dramatic intensity of the shock is expressed in the abundance of stishovite and high-pressure silica glass compared to other shergottites (Chennaoui *et al.*, unpubl. data).

Mineral Compositions

Pyroxenes–Pigeonite and augite are present as separate crystals with no pyroxenes of intermediate compositions (Figs. 3 and 6; Table 1). Augite crystals are euhedral to subhedral and display simple zoning towards Fe-rich rims.

Their FeO/MnO ratios are similar to those of shergottites (FeO/MnO = 32 ± 12 (2σ), n = 20) and correlate with their Mg number ($mg\#$ = Mg/(Mg + Fe) mole fraction) from 26 at $mg\#$ = 0.7 to 40 at $mg\#$ = 0.35. Augites range from $En_{45}Fs_{22}Wo_{32}$ to rims of $En_{27}Fs_{41}Wo_{32}$. Pigeonite grains are also euhedral to subhedral. They exhibit FeO/MnO = 34 ± 10 (2σ, n = 105), and range from $En_{59}Fs_{29}Wo_{12}$ to $En_{26}Fs_{59}Wo_{15}$. No extreme Fe-enriched compositions have been encountered. It should be noted that the cores of pigeonite and augite crystals have similar $mg\#$ values (~0.7), indicating contemporaneous nucleation. Their average compositions are strikingly close to those of Shergotty and Zagami (Table 2).

Abundances of the minor elements Al, Ti, Mn and Cr are also zoned from pyroxene cores to rims in a continuum, suggesting that the pyroxenes grew in a fractionating closed system (Fig. 7). Abundances of Ti and Mn increase from pyroxene cores to rims, while abundances of Cr decrease. This is in accord with their chemical behavior as incompatible *vs.* compatible elements. The case of Na is not as clear, possibly because of the limited variations in $mg\#$ compared to other

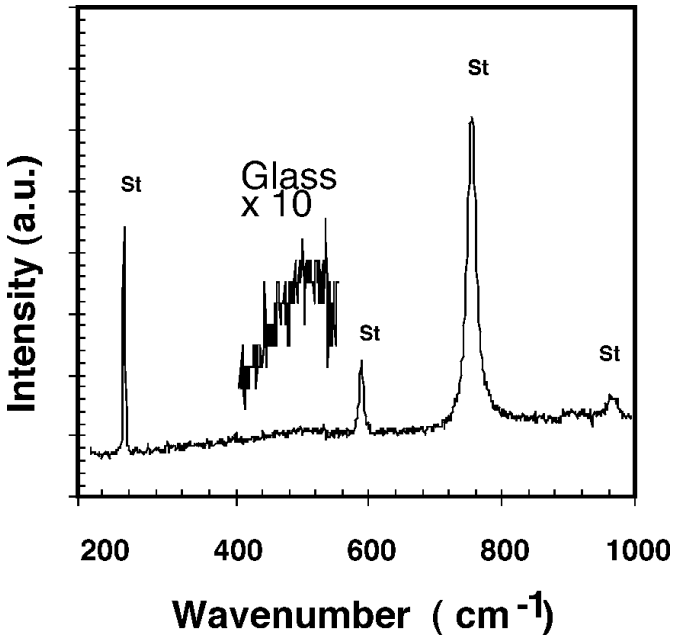

FIG. 5. Raman spectrum of a silica patch. The characteristic peaks at 231 and 753 cm^{-1} identify stishovite without ambiguity. A broad peak between 300 and 500 cm^{-1} corresponds to dense silica glass. The abundance of glass and its density (from the peak position) is variable from one spot to the next.

shergottites, and the comparatively small amount of Na in pyroxene with regard to analytical precision. In addition at low *mg#* , Na may be contaminated by maskelynite since these compositions correspond to pyroxene rims. The case of Al is particularly interesting as its concentration increases in the core of pyroxene and decreases for *mg#* below 0.56. This behavior can be explained as the fingerprint of plagioclase crystallization, in agreement with textural relationships.

We examined the pyroxenes at high magnification by field effect gun-scanning electron microscopy (FEG-SEM) in order to detect exsolution features. Preliminary results show that pyroxenes are devoid of exsolutions, at least on the scale of a few tens of nanometers. We find no evidence of exsolution in the Mg-rich cores and in the augite bands. The only exsolution-bearing areas are located in pyroxenes in contact with the melt pockets.

Maskelynites–Plagioclase has been converted into maskelynite by shock, as in other shergottites. Maskelynite areas are interstitial to pyroxenes and typically lath-shaped. They display small offshoots as smooth and irregular branches in the neighboring pyroxenes, and commonly contain pyroxene fragments that were rafted into the maskelynite. The maskelynite is normally zoned ($An_{35–53}Ab_{56–42}Or_{1–5}$, with an average of $An_{50}Ab_{48}Or_2$; Table 3), similar to maskelynite in Shergotty and Los Angeles (Hale *et al.*, 1999; Rubin *et al.*,

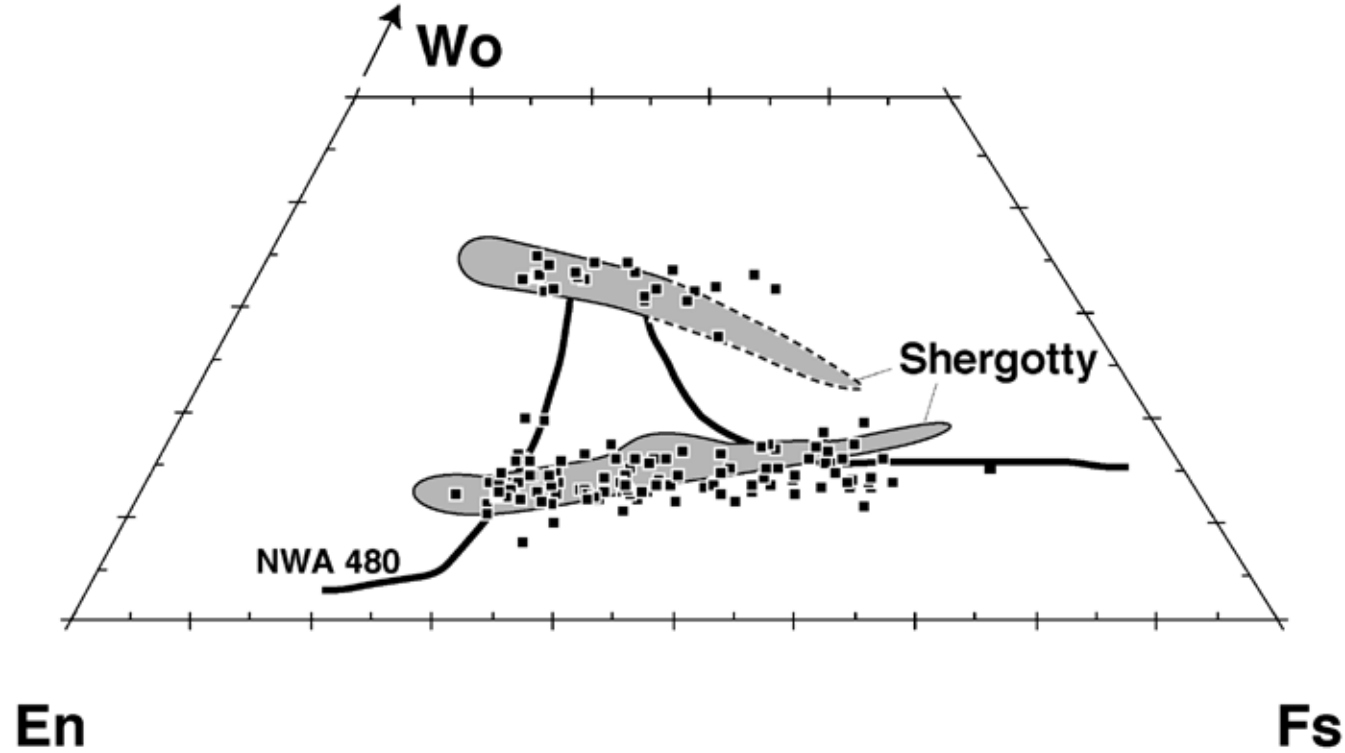

FIG. 6. Quadrilateral pyroxene compositions of NWA 856 compared to Shergotty (shaded area). Data sources are Stöffler *et al.* (1986), Stolper and McSween (1979), and Smith and Hervig (1979). The line corresponds to the zoning trend observed in shergottite NWA 480 (Barrat *et al.*, 2002).

TABLE 1. Representative electron microprobe analyses of NWA 856 pyroxenes. FeO* = total Fe.

	49	291	35	52	423	371	44	362
Pigeonite								
SiO_2	52.85	52.78	51.88	51.41	50.67	49.75	49.52	48.62
TiO_2	0.19	0.16	0.16	0.35	0.19	0.45	0.56	0.72
Al_2O_3	0.67	1.78	0.78	0.78	0.69	0.63	0.64	0.85
Cr_2O_3	0.44	0.33	0.42	0.24	0.09	0.11	0.10	0.08
FeO*	17.46	20.24	24.19	25.17	29.29	29.93	31.58	34.48
MnO	0.75	0.69	0.60	0.67	0.80	0.81	0.62	0.94
MgO	20.27	17.66	15.95	14.92	12.97	11.12	9.43	7.91
CaO	6.33	6.04	5.70	6.17	5.22	6.54	7.18	5.75
Na_2O	0.10	0.29	0.11	0.12	0.07	0.07	0.08	0.11
K_2O	0.04	0.03	0.00	0.00	0.00	0.00	0.00	0.01
P_2O_5	0.21	0.03	0.04	0.09	0.00	0.04	0.07	0.02
Cr_2O_3	0.44	0.33	0.42	0.24	0.09	0.11	0.10	0.08
Total	99.30	100.06	99.84	99.91	99.98	99.45	99.77	99.49
En	0.59	0.53	0.47	0.45	0.39	0.34	0.29	0.25
Fs	0.28	0.34	0.40	0.42	0.50	0.51	0.55	0.62
Wo	0.13	0.13	0.12	0.13	0.11	0.14	0.16	0.13
	28	31	24	402	407	340	20	
Augite								
SiO_2	52.34	51.60	51.53	51.47	50.98	50.09	50.04	
TiO_2	0.19	0.20	0.21	0.36	0.34	0.49	0.54	
Al_2O_3	1.05	1.14	1.27	1.16	1.14	1.01	0.97	
Cr_2O_3	0.46	0.84	0.54	0.33	0.37	0.29	0.11	
FeO*	13.84	14.95	16.15	17.50	21.33	23.79	23.59	
MnO	0.41	0.57	0.56	0.58	0.65	0.63	0.59	
MgO	15.51	15.06	13.52	12.24	11.18	10.80	8.82	
CaO	15.67	15.04	16.20	15.84	13.99	12.42	15.04	
Na_2O	0.18	0.26	0.17	0.18	0.13	0.16	0.20	
K_2O	0.04	0.00	0.00	0.01	0.00	0.00	0.04	
P_2O_5	0.16	0.24	0.31	0.01	0.06	0.00	0.24	
Cr_2O_3	0.46	0.84	0.54	0.33	0.37	0.29	0.11	
Total	99.84	99.89	100.47	99.67	100.23	99.68	100.16	
En	0.45	0.44	0.39	0.37	0.34	0.33	0.27	
Fs	0.22	0.24	0.26	0.29	0.36	0.40	0.40	
Wo	0.33	0.32	0.34	0.34	0.30	0.27	0.33	

TABLE 2. Composition of average pyroxene cores in NWA 856 (this study), Shergotty (Hale, 1999), and Zagami (McCoy *et al.*, 1992).

	NWA 856 (This study)		Shergotty (Hale, 1998)		Zagami (McCoy *et al.*, 1992)	
	Pigeonite	Augite	Pigeonite	Augite	Pigeonite	Augite
SiO_2	53.4	52.6	52.8	51.9	53.0	51.7
TiO_2	0.12	0.21	0.14	0.17	0.15	0.22
Al_2O_3	0.70	1.05	0.72	1.27	0.78	1.20
Cr_2O_3	0.46	0.68	0.50	0.71	0.45	0.71
FeO*	18.1	13.4	17.8	12.2	19.2	12.9
MnO	0.63	0.51	0.64	0.50	0.63	0.44
MgO	20.3	15.4	20.6	16.4	20.7	15.8
CaO	6.29	15.85	6.36	16.20	5.60	16.10
Na_2O	0.09	0.18	0.08	0.17	0.10	0.18
Total	100.0	99.9	99.6	99.5	100.6	99.3
En	*58.0*	*44.9*	*58.6*	*47.0*	*58.3*	*45.7*
Wo	*12.9*	*33.2*	*13.0*	*33.4*	*11.3*	*33.4*
Fs	*29.0*	*21.9*	*28.4*	*19.6*	*30.3*	*20.9*

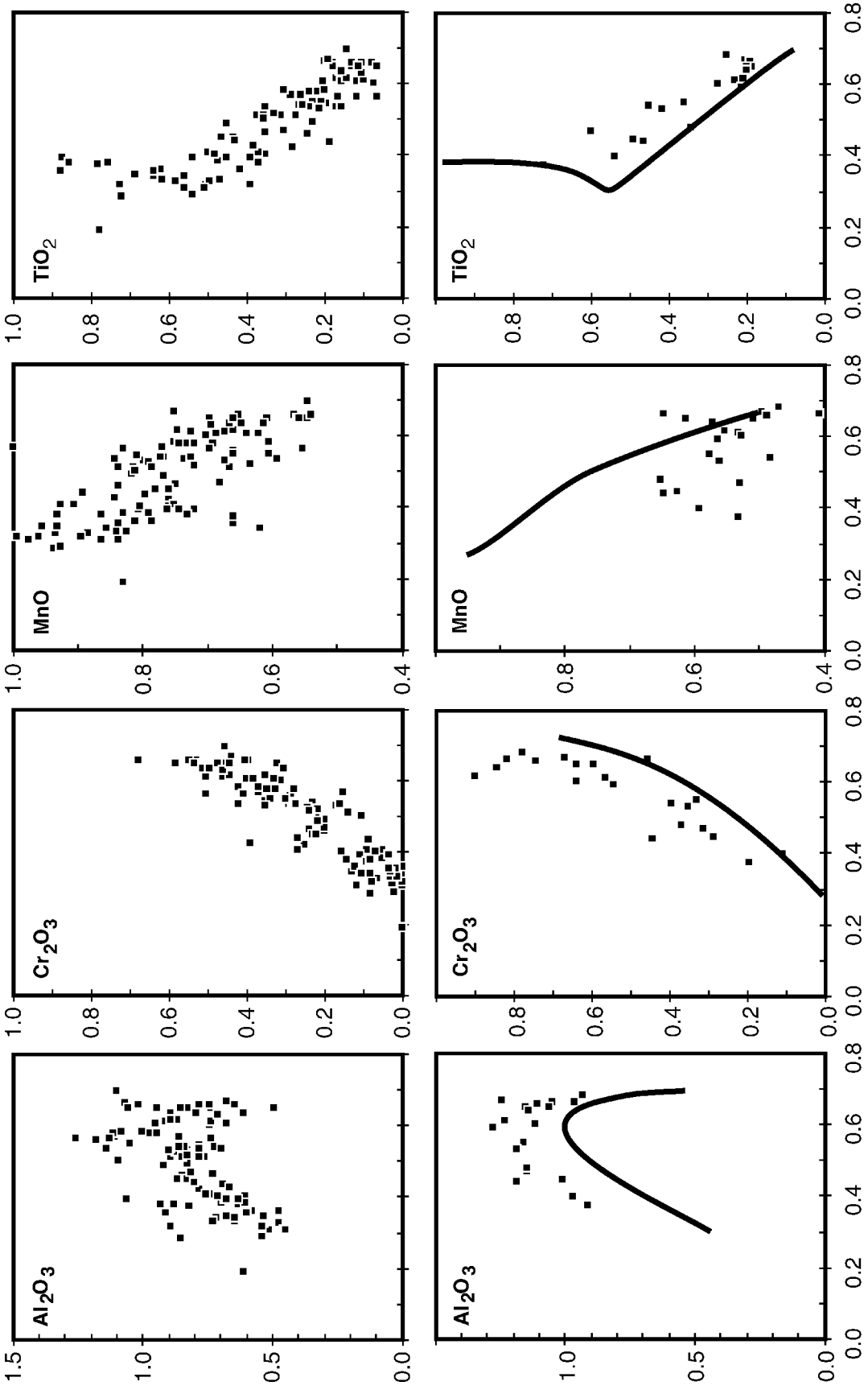

FIG. 7. Co-variations of Al_2O_3, Cr_2O_3, MnO and TiO_2 with *mg#* in NWA 856 pyroxenes. All oxides in wt%. (Top) pigeonites, (bottom) augites. Lines are average trend in pigeonites.

TABLE 3. Representative electron microprobe analyses of NWA 856 maskelynite, silica, and maskelynite–silica mixtures.

	Maskelynite							Silica	
	269	270	193	60	12	Moyenne	σ	T50	T44
SiO_2	61.03	58.65	57.76	56.80	55.52	55.39	0.33	95.98	99.04
TiO_2	0.00	0.06	0.09	0.06	0.12	0.05	0.06	1.32	0.13
Al_2O_3	24.08	25.28	25.02	25.46	27.83	27.63	0.31	0.06	0.67
Cr_2O_3	0.00	0.04	0.23	0.00	0.00	0.10	0.11	0.09	0.00
FeO*	0.80	0.49	0.85	1.02	0.81	0.94	0.17	1.22	0.10
MnO	0.00	0.00	0.18	0.00	0.03	0.12	0.09	0.00	0.03
MgO	0.09	0.01	0.03	0.08	0.04	0.05	0.03	0.03	0.00
CaO	7.36	8.11	9.05	10.13	10.93	10.76	0.10	0.06	0.04
Na_2O	6.10	6.22	5.75	5.66	4.86	5.10	0.19	0.00	0.28
K_2O	0.64	0.80	0.65	0.22	0.37	0.35	0.06	0.02	0.11
P_2O_5	0.14	0.06	0.09	0.18	0.21	0.17	0.07	0.00	0.11
Total	100.22	99.72	99.68	99.60	100.72	100.65	0.52	98.78	100.49
Ab	0.53	0.54	0.51	0.50	0.42	0.045	–	–	–
An	0.35	0.39	0.44	0.49	0.53	0.52	–	–	–
Or	0.04	0.05	0.04	0.01	0.01	0.02	–	–	–
Qz	0.09	0.02	0.02	0.00	0.03	0.01	–	–	–

	K-feldspar silica mixtures			Maskelynite–silica mixtures							
	T52	G52	T35	235	233	231	204	256	222	185	260
SiO_2	71.76	76.11	85.82	55.93	60.62	67.00	71.02	74.70	79.90	84.23	94.01
TiO_2	0.11	0.03	0.16	0.00	0.00	0.00	0.04	0.18	0.27	0.13	0.20
Al_2O_3	15.76	13.16	6.42	27.02	24.29	20.62	18.23	12.98	12.07	9.84	3.38
Cr_2O_3	0.00	0.04	0.00	0.00	0.09	0.00	0.00	0.28	0.00	0.00	0.00
FeO*	0.31	0.43	0.22	0.60	0.71	0.40	0.59	0.30	0.40	0.57	0.15
MnO	0.01	0.14	0.13	0.00	0.18	0.03	0.03	0.00	0.10	0.00	0.00
MgO	0.02	0.00	0.00	0.00	0.05	0.04	0.05	0.06	0.04	0.01	0.00
CaO	0.97	0.83	0.25	10.24	9.04	7.22	6.02	5.78	3.50	2.57	0.71
Na_2O	2.07	2.41	1.10	5.28	4.69	4.31	4.25	3.34	3.26	3.08	1.05
K_2O	9.25	6.73	3.94	0.46	0.40	0.31	0.42	0.42	0.29	0.29	0.24
P_2O_5	0.05	0.20	0.07	0.04	0.13	0.14	0.15	1.87	0.09	0.00	0.00
Total	100.31	100.08	98.10	99.57	100.19	100.06	100.79	99.89	99.91	100.73	99.73
Ab	0.18	0.20	0.09	0.46	0.41	0.37	0.35	0.28	0.27	0.25	0.08
An	0.05	0.04	0.01	0.50	0.43	0.34	0.28	0.27	0.16	0.11	0.03
Or	0.52	0.38	0.22	0.03	0.02	0.02	0.02	0.02	0.02	0.02	0.01
Qz	0.25	0.38	0.68	0.01	0.14	0.28	0.34	0.42	0.56	0.62	0.87

2000). Notice that because of the analytical spot size (10 μm), zoning may actually have a wider range than that measured. They contain a moderate amount of Fe (FeO = 0.94 ± 0.17 (1σ), n = 102), similar to that in Shergotty maskelynites. In a few areas, glass with K-feldspar composition has been detected. In addition, significant phosphorus appears in most EMP analyses (P_2O_5 = 0.17 ± 0.07 (1σ), n = 102). We suggest that P is dissolved in the lattice or that maskelynite contains tiny phosphate inclusions.

Baddeleyite–Two small crystals of baddeleyite were recognized, one of which could be analyzed. Its chemical composition is ZrO_2 = 98.02, HfO_2 = 1.14, SnO_2 = 0.08 ± 0.03, SiO_2 = 0.05 wt%. This grain has a Zr/Hf ratio of 74, which is nearly twice that of the bulk rock. Baddeleyite has been reported in Shergotty, QUE 94201 and Los Angeles (Smith and Hervig, 1979; Lundberg *et al.*, 1988; McSween *et al.*, 1996; Rubin *et al.*, 2000).

Phosphates–Merrillite and Cl-apatite are present in NWA 856 (Table 4). Merrillite, the most abundant phosphate, occurs as thin laths (up to 0.1 mm in length) and contains a moderate amount of FeO (3.2 ± 0.2 wt%). Merrillite grains are often associated with silica, Fe-Ti oxides, pyrrhotite and fayalite.

TABLE 4. Representative electron microprobe analyses of NWA 856 minor mineral phases.

	Pyroxene cores Spinel		Interstitial ilmenite	Interstitial ulvöspinel	Melt pockets			Merrilite
	78	74	6	8	424	359	395	4
SiO_2	0.07	0.82	0.00	0.11	57.13	53.69	49.81	0.35
TiO_2	22.83	18.12	51.49	23.54	0.00	0.54	0.48	0.02
Al_2O_3	1.66	6.41	0.01	1.74	25.86	15.30	8.27	0.05
Cr_2O_3	2.99	10.04	0.12	0.70	0.00	0.26	0.08	0.00
FeO*	67.21	59.54	46.52	70.73	1.07	12.80	15.43	2.94
MnO	0.42	0.50	0.40	0.58	0.03	0.27	0.05	0.22
MgO	0.41	0.75	0.79	0.32	0.04	4.42	8.67	1.93
CaO	0.19	0.52	0.00	0.00	9.69	9.39	13.50	45.38
Na_2O	0.00	0.03	0.02	0.20	5.08	2.67	1.69	1.43
K_2O	0.00	0.01	0.00	0.00	0.35	0.27	0.00	0.05
P_2O_5	0.00	0.00	0.00	0.00	0.22	0.20	0.35	45.24
Total	95.776	96.73	99.35	97.91	99.46	99.81	98.33	97.59

Opaque Minerals–Ulvöspinel (Fe/Ti ≈ 3.4) is the most abundant opaque mineral (Table 4); it is interstitial among pyroxenes and maskelynite, and often is rimmed with ilmenite. At high magnification, the ulvöspinel crystals appear heterogeneous at a scale of a few micrometers. They frequently contain small rounded inclusions of silica, both stishovite and glass, which are commonly surrounded by radial cracks. Unlike in NWA 480, Cr-spinel crystals are small and rare in the pyroxene cores; their chromite component is moderate. Small pyrrhotite crystals are rare (Fe = 59.36 wt%, Ni = 0.29 wt%, S = 37.65 wt%).

Silica–Electron microprobe analyses (Table 3) show that this phase is free of aluminum, unlike the silica grains in Shergotty, Zagami and NWA 480 (Stolper and McSween, 1979; Sharp *et al.*, 1999; Weber *et al.*, 2000; Barrat *et al.*, 2001). Its textural relationship with maskelynite indicates that the silica marks boundaries of the original plagioclase crystals. The original silica was interstitial among plagioclase and pyroxene. Backscattered electron images show that silica is not homogenous: some stishovite has retrograded to glass as shown by Raman spectroscopy.

Even more interesting is the chemical relationship between maskelynite and silica. Intermediate compositions are common but, surprisingly, the most common composition is SiO_2 = 80–75% (Fig. 8). Silica rich glass has been mentioned previously in Shergotty, QUE 94201 and ALH 84001 (Binns, 1967; Smith and Hervig, 1979; Stolper and McSween, 1979; McSween *et al.*, 1996; Thomas *et al.*, 1996). Contribution of a pyroxene component is obvious for a few points only. A similar observation can be made in a few instances for a mixture between silica and K-feldspar composition. We suggest that such intermediate compositions are eutectic-like composition in the plagioclase–silica and K-feldspar silica systems. The silica–maskelynite system is a ternary (Qz–Ab–An) and melts are enriched in Ab relative to the solid assemblage. A trend towards an Ab-enriched composition is observed, a deviation from a simple binary mixing between maskelynite and silica. This suggests that shock promoted melting at silica–feldspar boundaries where minimum transport distance by diffusion is required, with the eutectic composition corresponding to the maximum extent of melting; the time allowed above the transformation temperature was so short that some silica was preserved and in a water-free system (or nearly so), the kinetics was too sluggish to permit feldspar and silica crystallization upon cooling.

Amphibole–The pyroxene cores of NWA 856 sometimes contain small melt inclusions with amphibole, pyrrhotite and K-feldspar like those of Shergotty and Zagami (Treiman, 1985; McCoy *et al.*, 1992). In our section, amphiboles are too small to be accurately analyzed. An amphibole analysis has been obtained with another section and corresponds to a kaersutite (Mikouchi and Monkawa, pers. comm.).

Impact Melt Pockets–Melt pockets are typically from 0.5 to 2 mm in diameter. Analysis with a 10 μm spot shows that the average melt composition, though heterogeneous, corresponds to a mixture of maskelynite and pyroxene (Fig. 9 and Table 5). Ghost minerals, like maskelynite or pyroxene lumps, can still be recognized. In addition stishovite is identified either as rounded clots or polygonal spots of 100–300 μm and always associated with variable amounts of dense silica glass. Nearby are numerous submicron needles of stishovite with square cross sections. The phosphorus content of the melt pockets is low (0.22% on the average with a maximum of 0.45).

Carbonates–On the section examined, a few large fractures cross cutting the fusion crust (see Fig. 2), appear to be coated with fluffy material. The determination of this material as calcium carbonate was possible with EDS analysis (including the detection of C). No other products of terrestrial alteration were visible.

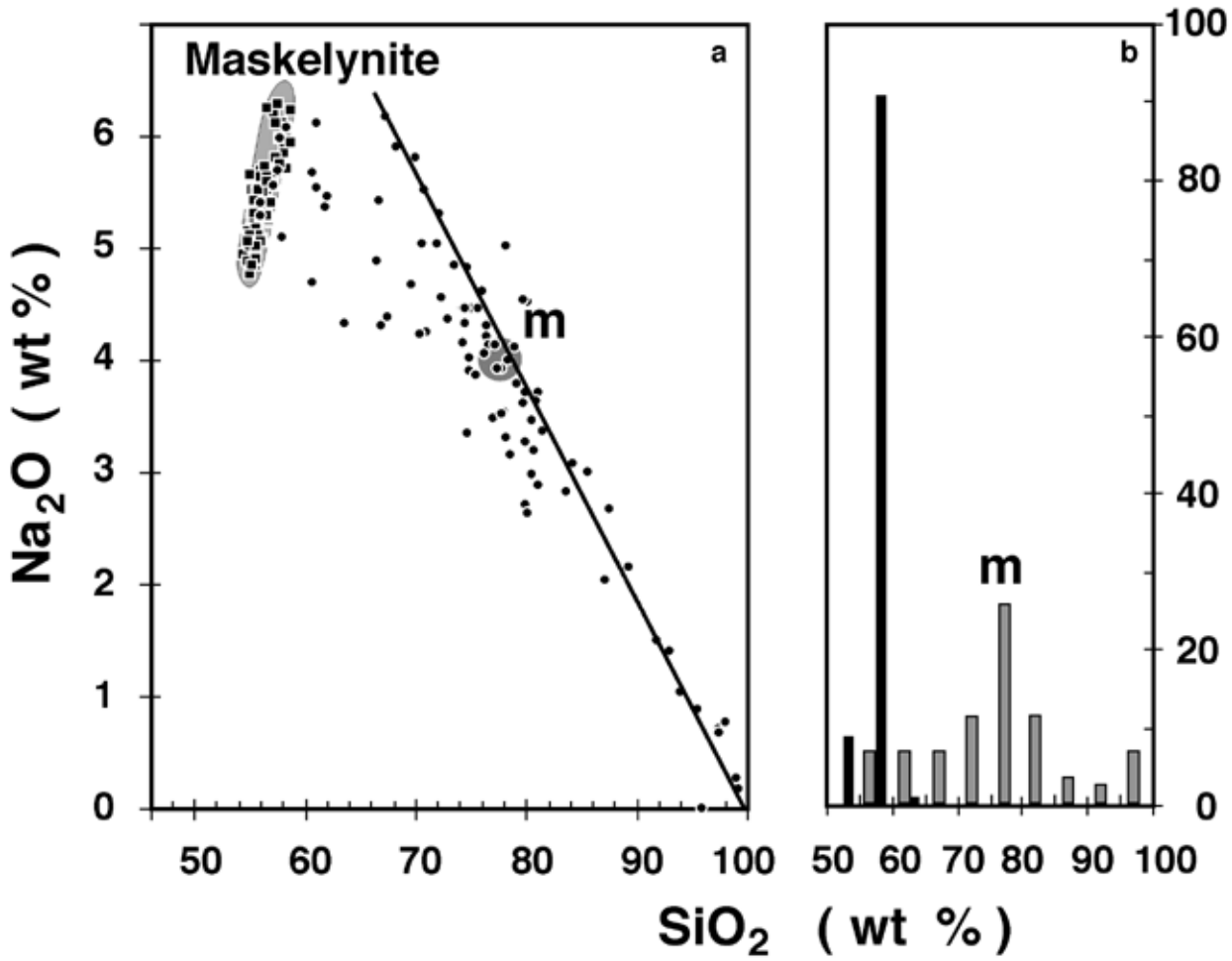

FIG. 8. Composition of silica-maskelynite patches associated with maskelynite. (a) The straight line is a visual fit to the SiO_2 > 80% data points. For SiO_2 < 80%, some of the data points correspond to a mixture of maskelynite and some component (**m**) at 80% silica; they are likely to be an artifact related to the size of the analytical spot (10 μm). The trend to a sodium-rich component (the straight line) is expected for a melt derived from silica and maskelynite. (b) The histogram of SiO_2 concentrations reveals, beside maskelynite, a subsidiary maximum corresponding to the most likely melt composition (**m**) in the plagioclase–silica system.

Bulk Chemistry

The bulk composition of NWA 856 is given in Table 5. This new shergottite is an Al-poor ferroan basaltic rock which strongly resembles Shergotty and Zagami in its major element composition. Major element ratios such as FeO*/MnO (=36), where FeO* is total iron, or Na/Al (=0.26) are typical of shergottites (McSween, 1994). In a Cr *vs. mg#* diagram, NWA 856 falls exactly on the Shergotty–Nakhla–Chassigny (SNC) trend which departs markedly from terrestrial, howardite–eucrite–diogenite (HED) or lunar trends (Fig. 10).

Alteration–Because hot desert alteration can affect the compositions of meteorites (*e.g.*, Bland *et al.*, 1998; Barrat *et al.*, 1998, 1999, 2001; Stelzner *et al.*, 1999; Zipfel *et al.*, 2000; Crozaz and Wadhwa, 2001), these effects must be evaluated. Chemical effects of alteration should be most obvious in abundances of Ba, Sr, Cs, U and Ce (Table 6). NWA 856 has a chondritic Th/U ratio (=4.1), similar to the ratios in the unweathered falls Shergotty and Zagami. Hot desert meteorites often display a strong Ba and Sr enrichment (*e.g.*, Stelzner *et al.*, 1999; Folco *et al.*, 2000), especially when secondary carbonates are present. Ba and Sr abundances in NWA 856 are in the trend defined by other "unweathered" shergottites (Fig. 11). In a few Saharan finds, elevated Cs abundances have been measured (*e.g.*, Folco *et al.*, 2000). The Cs/Th ratio of NWA 856 (~1.1) is similar to those of Zagami and Shergotty (1.3 and 1.4, respectively). Barrat *et al.* (1999) and Neal *et al.* (2001) have shown that desert weathering is able to produce a significant positive Ce anomaly. The slight positive Ce anomaly of NWA 856 (Ce/Ce* = 1.01) is barely significant (Fig. 12). Therefore, alteration effects on the bulk composition of NWA 856 are negligible especially when compared to DaG 476–489 and Dhofar 019.

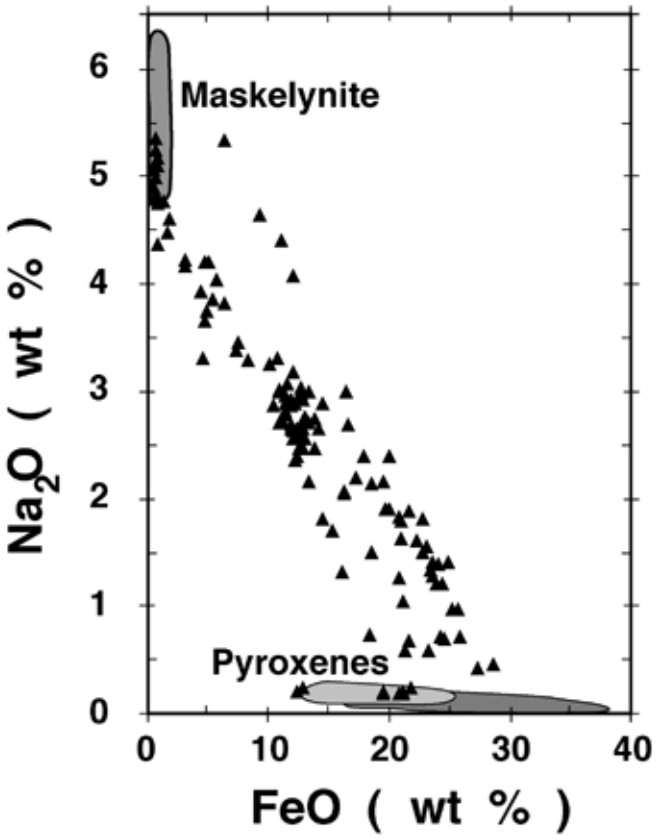

FIG. 9. Systematic analysis of impact melt pockets reveal (besides residual pyroxene and maskelynite) a simple binary mixture of maskelynite and pyroxene, the two dominant phases in the rock.

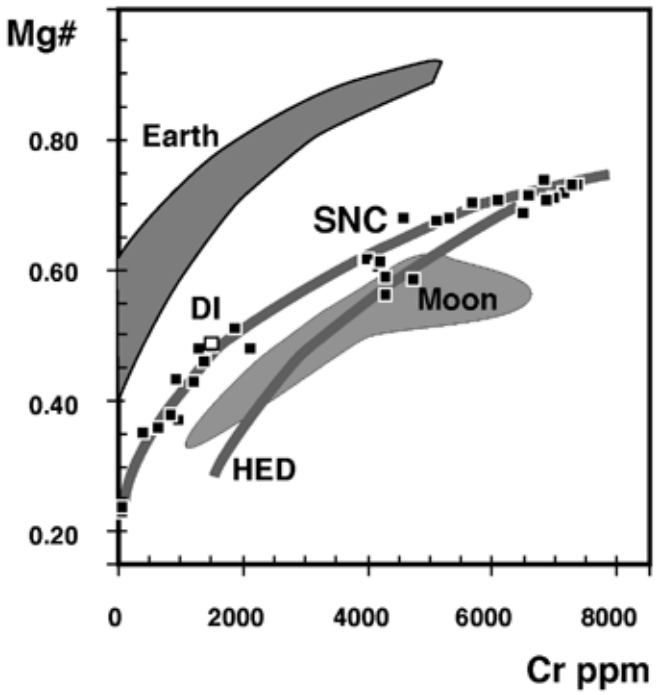

FIG. 10. In a Cr *vs. mg#* plot, SNC meteorites follow a well-defined fractionation trend that departs markedly from terrestrial, lunar and HED evolutions. NWA 856 falls exactly on this trend demonstrating its consanguinity with SNC meteorites.

TABLE 5. Major element abundances (in wt%) for NWA 856 compared to NWA 480 (Barrat *et al.*, 2002), Zagami and Shergotty (Stolper and McSween, 1979), and Los Angeles.

	NWA 856		Zagami Stolper and McSween (1979)	Shergotty Stolper and McSween (1979)	NWA 480 Barrat *et al.* (2002)	Los Angeles ICP/AES (This study)
	ICP/AES (This study)	INAA (This study)				
SiO_2			50.8	50.4	–	–
TiO_2	0.81	–	0.77	0.81	1.16	1.12
Al_2O_3	6.83	–	5.67	6.89	6.46	10.86
Cr_2O_3	0.23	0.27	0.30	0.21	0.31	0.015
FeO*	17.81	19.97	18.0	19.1	19.44	21.07
MnO	0.49	0.54	0.50	0.50	0.51	0.46
MgO	9.51	–	11.0	9.27	10.06	3.91
CaO	10.24	–	10.8	10.1	9.32	9.92
Na_2O	1.28	–	0.99	1.37	1.26	2.24
K_2O	0.13	–	0.14	0.16	0.10	0.36
FeO*/MgO	1.87	–	1.64	2.06	1.93	5.39
FeO*/MnO	36.35	36.98	36.00	38.20	38.12	45.72
Al_2O_3/TiO_2	8.43	–	7.36	8.51	5.57	9.72
TiO_2/Na_2O	0.63	–	0.78	0.59	0.92	0.50

TABLE 6. Trace element abundances (in ppm) for NWA 856, Zagami, Shergotty, NWA 480 (Treiman, 1986; Barrat *et al.*, 2001, 2002), and Los Angeles.

	NWA 856		Zagami		Shergotty		NWA 480	Los Angeles
	ICP-MS	INAA	Treiman (1986)	Barrat *et al.* (2001)	Treiman (1986)	Barrat *et al.* (2001)	Barrat *et al.* (2002)	(This study)
Li	4.06	–	–	–	–	–	2.93	5.03
Be	0.355	–	–	–	–	–	0.21	0.54
Sc	55.7	54.1	–	53	–	54	28	41.3
V	295	–	–	–	–	–	202	–
Co	36.3	43	–	39.5	–	35	37.6	29.2
Ni	77	85	90	101	55	66	63	32
Cu	14.0	–	–	14.0	–	12.3	17.6	22.6
Zn	59.1	66	63.8	59	68.3	61	64	62.3
Ga	14.66	–	–	12.68	–	14.31	16.27	22.09
As	–	0.18	–	–	–	–	–	–
Br	–	2.64	0.79	–	1.06	–	–	–
Rb	6.24	8.2	9.56	5.32	9.5	5.57	2.67	12.00
Sr	48.7	56	–	38	–	40	49.3	81.0
Y	18.81	–	–	13.55	–	14.26	16.46	29.39
Zr	62.8	69	–	61.01	–	59.65	58.74	79.6
Nb	3.37	–	–	3.93	–	2.68	1.99	4.99
Ag	–	<0.05	0.0142	–	0.0169	–	–	–
Sb	–	0.014	0.0052	–	0.0017	–	–	–
Cs	0.43	0.41	0.367	0.37	0.529	0.42	0.19	0.88
Ba	41.3	46	–	22.3	–	25.6	28.4	46.8
La	2.16	2.34	–	1.44	–	1.56	1.48	3.97
Ce	5.49	6.1	–	3.47	–	3.73	3.77	9.84
Pr	0.786	–	–	0.509	–	0.568	0.619	1.43
Nd	3.88	3.9	–	2.53	–	2.97	3.70	7.07
Sm	1.50	1.68	–	0.961	–	1.18	1.73	2.64
Eu	0.582	0.62	–	0.399	–	0.479	0.756	1.02
Gd	2.51	–	–	1.56	–	1.94	2.67	4.28
Tb	0.474	0.48	–	0.308	–	0.381	0.477	0.792
Dy	3.12	–	–	2.17	–	2.53	3.05	5.04
Ho	0.677	–	–	0.479	–	0.548	0.62	1.03
Er	1.87	–	–	1.34	–	1.52	1.57	2.76
Yb	1.64	1.76	–	1.22	–	1.32	1.33	2.35
Lu	0.251	–	–	0.186	–	0.202	0.19	0.331
Hf	1.55	2.01	–	1.54	–	1.63	1.64	2.19
Ta	0.16	0.23	–	0.19	–	0.17	0.10	0.28
W	0.43	0.52	–	–	–	0.19	0.34	0.66
Au	–	0.004	0.00176	–	0.005	–	–	–
Pb	0.46	–	–	–	–	–	0.37	1.12
Th	0.398	0.442	–	0.285	–	0.293	0.215	0.57
U	0.096	0.092	0.094	0.075	0.129	0.068	0.064	0.12
$(La/Sm)_n$	0.91	0.88	–	0.94	–	0.83	0.54	0.95
Eu/Eu*	0.92	–	–	1.00	–	0.97	1.08	0.93

Comparison with Other Shergottites–Many element ratios have been used in order to discriminate the various types of basaltic achondrites (for a review, see Treiman *et al.*, 2000). Trace element ratios such as K/La (=500) or Ga/Al ($= 4.8 \times 10^{-4}$) indicate clearly that NWA 856 is a new member of the martian meteorite clan. This conclusion is confirmed by the bulk rock analysis for oxygen isotopes which yields $\delta^{17}O = +3.09‰$, $\delta^{18}O = +5.03‰$, $\Delta^{17}O = +0.47‰$, a value slightly higher than those measured on other shergottites (Clayton and Mayeda, 1983, 1996; Romanek *et al.*, 1998; Franchi *et al.*, 1999) but

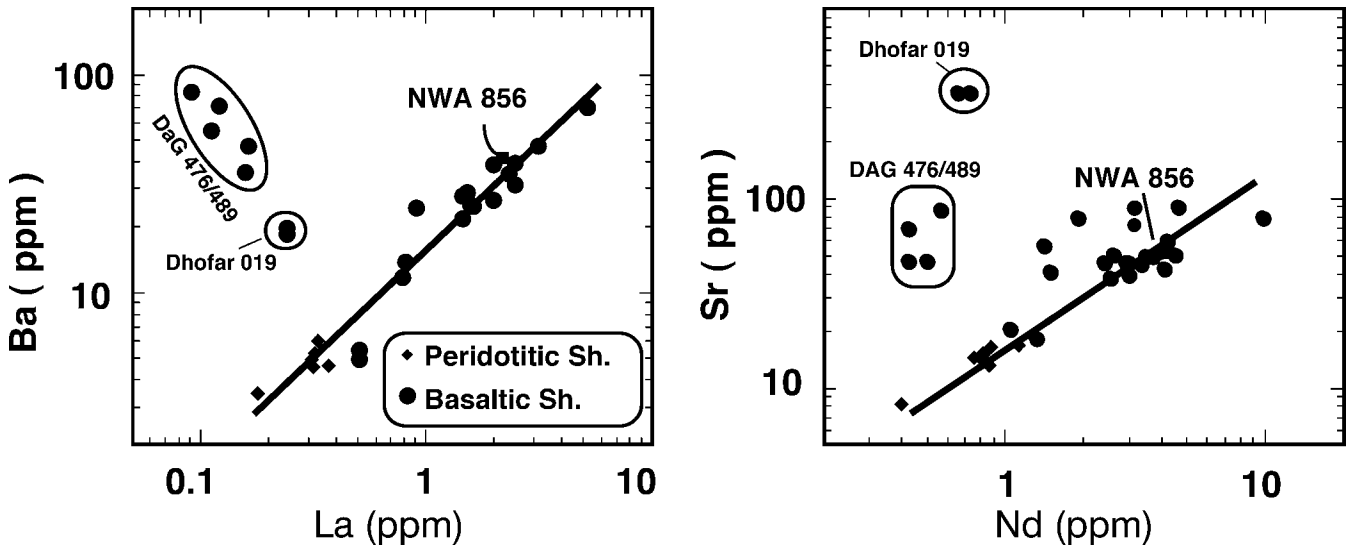

FIG. 11. Concentrations of Ba and Sr *vs.* La and Nd in shergottites. Unlike NWA 856, both Dhofar 019 and Dar al Gani 476/489 display strong Ba and Sr enrichment, a feature of hot desert weathering. Literature data are from Barrat *et al.* (2001, 2002), Borg *et al.* (2000), Burghele *et al.* (1983), Dreibus *et al.* (1982, 1992, 1996), Folco *et al.* (2000), Gleason *et al.* (1997), Jagoutz (1989), Jagoutz and Wänke (1986), Jérome (1970), Kong *et al.* (1999), Laul *et al.* (1986), Ma *et al.* (1981, 1982), Neal *et al.* (2001), Rubin *et al.* (2000), Shih *et al.* (1982), Smith *et al.* (1984), Treiman *et al.* (1994), Warren and Kallemeyn (1987, 1996), Warren *et al.* (1999), and Zipfel *et al.* (2000).

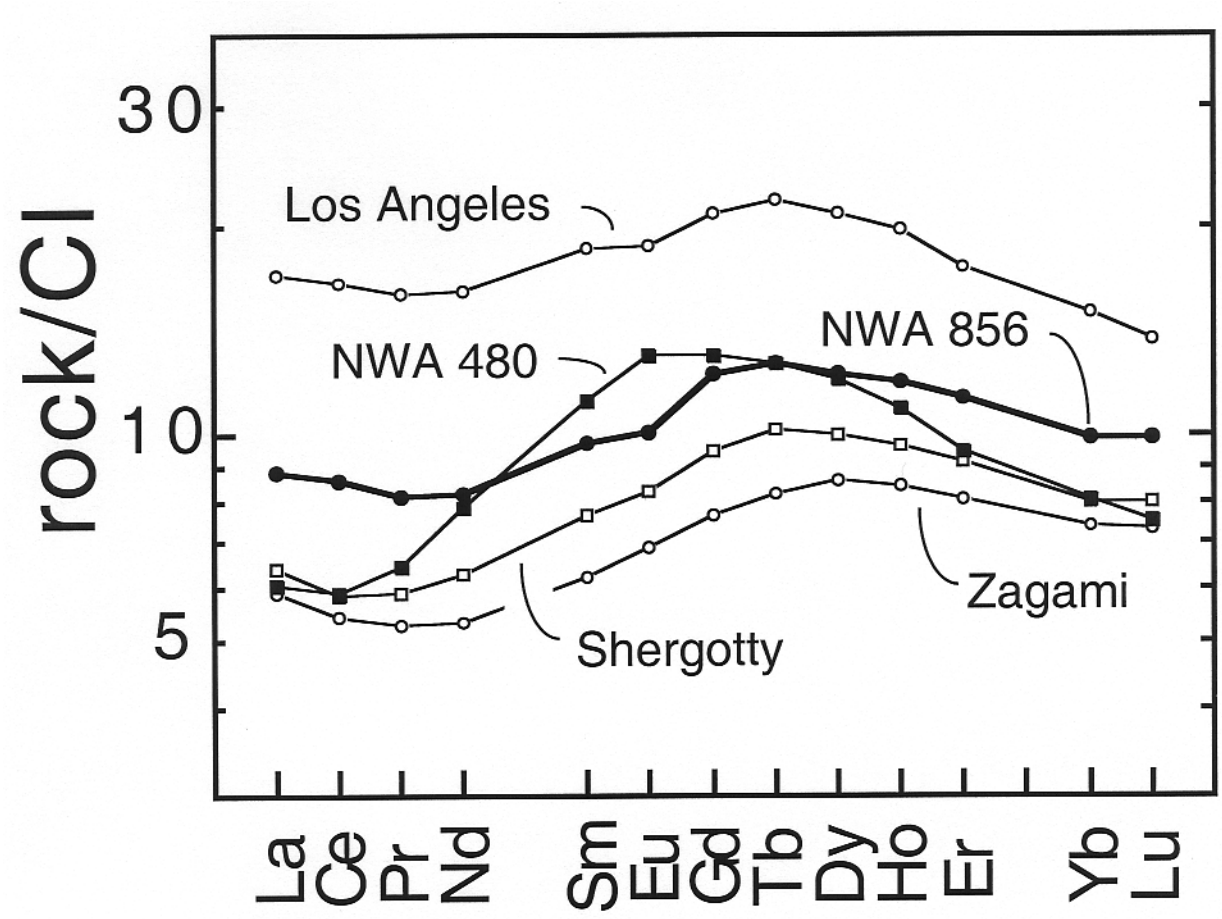

FIG. 12. REE pattern of NWA 856 compared to Zagami, Shergotty, NWA 480 and Los Angeles (Barrat *et al.*, 2001, 2002). The reference chondrite is from Evensen *et al.* (1978). Notice the strong similarity between NWA 856, Zagami, Shergotty and Los Angeles contrasting with the pattern of NWA 480.

compatible with the overall scatter of previous analyses of martian meteorites. Indeed, if we consider the data of Clayton and Mayeda (1983, 1996) the largest data base from one single laboratory, one obtains an average $\Delta^{17}O$ value of +0.31 when whole rocks alone are considered, with a 2σ range of ±0.1‰. If mineral separates are also considered then, the 2σ range becomes ±0.16‰. According to the $\Delta^{17}O$ value of NWA 480 (+0.4‰), another shergottite measured in the Paris laboratory, a calibration bias is likely to explain the high NWA 856 value in addition to the limited reproducibility of the technique.

Two determinations of trace element abundances were carried out on two different splits of the same powder using ICP-MS and INAA. The results are similar but not indistinguishable because of possible calibration bias (*e.g.*, Hf), and mainly because of powder heterogeneity. These differences should not be overemphasized. The compatible trace element abundances (such as Ni, Co, Cr, Cu) are strikingly similar to those reported for Shergotty and Zagami (Table 6). Furthermore, the rare earth element (REE) pattern of NWA 856 is parallel to those of Shergotty, Zagami and Los Angeles and obviously distinct from NWA 480. This is a strong evidence against pairing between NWA 480 and NWA 856 and a confirmation of its strong affinity with the Zagami and Shergotty meteorites.

CONCLUSIONS

NWA 856 is the second reported basaltic shergottite from Morocco after NWA 480. A number of arguments exclude the pairing of these two stones:

• The textures of the two rocks are different. Pyroxene phenocrysts and maskelynite laths are larger in NWA 480. The relationships between pyroxene and maskelynite on one hand and maskelynite and silica on the other are specific of NWA 856. The volume fraction and the size of impact melt pockets are significantly higher in NWA 856.

• NWA 856 exhibits two separate pyroxenes while NWA 480 pyroxene displays more complex zoning. Their compositions are significantly different. NWA 856 unlike NWA 480 is almost devoid of chromite in the core of its pyroxenes.

• NWA 856 and NWA 480 are chemically distinct. For example, the REE patterns of the two rocks are significantly different.

Among basaltic shergottites, Shergotty and Zagami strikingly resemble NWA 856 from phases and chemical perspectives. These three stones display similar bulk chemical compositions and contain pigeonite and augite in independent crystals, with similar core compositions (Table 2). Their REE are similar even though the REE concentrations of NWA 856 are 1.5× higher than in Zagami.

The crystallization conditions of such pyroxene assemblages in shergottites have been extensively discussed (Stolper and McSween, 1979; McCoy and Lofgren, 1999; McKay *et al.*, 2000; Dann *et al.*, 2001). Stolper and McSween (1979) and McCoy *et al.* (1992) have proposed that the textures observed in Shergotty and Zagami are indicative of a multi-stage magmatic history with Mg-rich pyroxene crystallization in a deep-seated magma chamber followed by eruption of a thick phenocryst-bearing lava flow. The magmatic conditions recorded by co-crystallization of augite and pigeonite crystals were recently inferred using experiments performed at various pressures, under anhydrous or H_2O-saturated conditions (Dann *et al.*, 2001), and estimated to 1120 °C and 56 MPa of a H_2O-saturated melt (~1.8 wt% in Shergotty parental melt). Crystallization under a significant vapor pressure is in agreement with the presence of amphibole inclusions in pyroxenes as observed in NWA 856, Shergotty and Zagami (Treiman, 1985; McCoy *et al.*, 1992). McSween *et al.* (2001) argue for a loss of water during the ascent of the magma, according to Li and B behaviors in Shergotty pyroxenes. The same crystallization history may be extended to the new shergottite NWA 856. The lack of mesostasis, the relative abundance of interstitial silica (previously quartz), K-feldspar glass (formerly K-feldspar) and mixtures of silica with maskelynite distinguish NWA 856 from Shergotty and Zagami, and suggest a slightly slower cooling at the end of the crystallization of NWA 856.

Acknowledgements–The authors are indebted to Carine Bidaut and Bruno Fectay for donating the NWA 856 sample and to Paul Warren (UCLA) for Los Angeles. Philippe Blanc and Choukri Derder helped with the SEM analyses in Paris. The CAMPARIS crew is acknowledged for assistance with EMPA. Dominique Badia processed some of the backscattered electron images. This research has made use of NASA's astrophysics data system abstract service. Thanks are due to the Progamme National de Planétologie (INSU) for financial support. Allan Treiman and an anonymous reviewer provided constructive reviews, which are appreciated.

Editorial handling: R. Korotev

REFERENCES

BARRAT J. A., GILLET PH., LECUYER CH., SHEPPARD S. M. F. AND LESOURD M. (1998) Formation of carbonates in the Tatahouine meteorite. *Science* **280**, 412–414.

BARRAT J. A., GILLET PH., LESOURD M., BLICHERT-TOFT J. AND POUPEAU G. R. (1999) The Tatahouine diogenite: Mineralogical and chemical effects of sixty-three years of terrestrial residence. *Meteorit. Planet. Sci.* **34**, 91–97.

BARRAT J. A., BLICHERT-TOFT J., GILLET PH. AND KELLER F. (2000) The differentiation of eucrites: The role of *in situ* crystallization. *Meteorit. Planet. Sci.* **35**, 1087–1100.

BARRAT J. A., BLICHERT-TOFT J., NESBITT R. W. AND KELLER F. (2001) Bulk chemistry of Saharan shergottite Dar al Gani 476. *Meteorit. Planet. Sci.* **36**, 23–29.

BARRAT J. A., GILLET PH., SAUTTER V., JAMBON A., JAVOY M., GÖPEL C., LESOURD M., KELLER F. AND PETIT E. (2002) Petrology and geochemistry of the basaltic shergottite Northwest Africa 480. *Meteorit. Planet. Sci*. **37**, 478–500.

BINNS R. W. (1967) Stoney meteorites bearing maskelynite. *Nature* **214**, 1111–1112.

BLAND P. A., SEXTON A. S., JULL A. J. T., BEVAN A. W. R., BERRY F. J., THORNLEY D. M., ASTIN T. R., BRITT D. T. AND PILLINGER

C. T. (1998) Climate and rock weathering: A study of terrestrial age dated ordinary chondrite meteorites from hot desert regions. *Geochim. Cosmochim. Acta* **62**, 3169–3184.

BLICHERT-TOFT J., GLEASON J. D., TÉLOUK P. AND ALBARÈDE F. (1999) The Lu-Hf isotope geochemistry of shergottites and the evolution of the martian mantle–crust system. *Earth Planet. Sci. Lett.* **173**, 25–39.

BORG L. E., NYQUIST L. E., TAYLOR L. A., WIESMANN H. AND SHIH C-Y. (1997) Rb-Sr and Sm-Nd isotopic analyses of QUE 94201: Constraints on martian differentiation processes (abstract). *Lunar Planet. Sci.* **28**, 133–134.

BORG L. E., NYQUIST L. E., WIESMANN H., REESE Y. AND PAPIKE J. J. (2000) Sr-Nd isotopic systematics of martian meteorite DaG 476 (abstract). *Lunar Planet. Sci.* **31**, #1036, Lunar and Planetary Institute, Houston, Texas, USA (CD-ROM).

BURGHELE A., DREIBUS G., PALME H., RAMMENSEE W., SPETTEL B., WECKWERTH G. AND WÄNKE H. (1983) Chemistry of shergottites and the shergottite parent body (SPB): Further evidence for the two components model for planet formation (abstract). *Lunar Planet. Sci.* **14**, 80–81.

CLAYTON R. N. AND MAYEDA T. K. (1983) Oxygen isotopes in eucrites, shergottites, nakhlites and chassignites. *Earth Planet. Sci. Lett.* **62**, 1–6.

CLAYTON R. N. AND MAYEDA T. K. (1996) Oxygen isotopic studies of achondrites. *Geochim. Cosmochim. Acta* **60**, 1999–2017.

CROZAZ G. AND WADHWA M. (2001) The terrestrial alteration of Saharan shergottites Dar al Gani 476 and 489: A case study of weathering in a hot desert environment. *Geochim. Cosmochim. Acta* **65**, 971–978.

DANN J. C., HOLZHEID A. H., GROVE T. L. AND MCSWEEN H. Y., JR. (2001) Phase equilibria of the shergotty meteorite: Constraints on pre-eruptive water contents of martian magmas and fractional crystallization under hydrous conditions. *Meteorit. Planet. Sci.* **36**, 793–806.

DREIBUS G., PALME H., RAMMENSEE W., SPETTEL B., WECKWERTH G. AND WÄNKE H. (1982) Composition of the Shergotty parent body: Further evidence for a two components model for planet formation (abstract). *Lunar Planet. Sci.* **13**, 186–187.

DREIBUS G., JOCHUM K. P., PALME H., SPETTEL B., WLOTZKA F. AND WÄNKE H. (1992) LEW 88516: A meteorite compositionally close to the "martian mantle" (abstract). *Meteoritics* **27**, 216–217.

DREIBUS G., SPETTEL B., WLOTZKA F., SCHULTZ L., WEBER H. W., JOCHUM K. P. AND WÄNKE H. (1996) QUE 94201: An unusual martian basalt (abstract). *Meteorit. Planet. Sci.* **31 (Suppl.)**, A39–A40.

EVENSEN N. M., HAMILTON P. J. AND O'NIONS R. K. (1978) Rare earth abundances in chondritic meteorites. *Geochim. Cosmochim. Acta* **42**, 1199–1212.

FOLCO L., FRANCHI I. A., D'ORAZIO M., ROCCHI S. AND SCHULTZ L. (2000) A new martian meteorite from the Sahara: The shergottite Dar al Gani 489. *Meteorit. Planet. Sci.* **35**, 827–839.

FRANCHI A., WRIGHT I. P., SEXTON A. S. AND PILLINGER C. T. (1999) The oxygen isotopic composition of Earth and Mars. *Meteorit. Planet. Sci.* **34**, 657–661.

GLEASON J. D., KRING D. A., HILL D. H. AND BOYNTON W. V. (1997) Petrography and bulk chemistry of martian lherzolite LEW 88516. *Geochim. Cosmochim. Acta* **61**, 4007–4014.

GROVE T. L. AND BENCE A. E. (1977) Experimental study of pyroxene-liquid interaction in quartz-normative basalt 15597. *Proc. Lunar Planet. Sci. Conf.* **8th**, 1549–1579.

HALE V. P. S., MCSWEEN H. Y., JR. AND MCKAY G. A. (1999) Re-evaluation of intercumulus liquid composition and oxidation state for the Shergotty meteorite. *Geochim. Cosmochim. Acta* **63**, 1459–1470.

JAGOUTZ E. (1989) Strontium and neodymium systematics in ALHA77005: Age of shock metamorphism in shergottites and magmatic differentiation on Mars. *Geochim. Cosmochim. Acta* **53**, 2429–2441.

JAGOUTZ E. (1991) Chronology of SNC meteorites. *Space Sci. Rev.* **56**, 13–22.

JAGOUTZ E. AND WÄNKE H. (1986) Sr and Nd isotopic systematics of Shergotty meteorite. *Geochim. Cosmochim. Acta* **50**, 939–953.

JÉROME D. Y. (1970) Composition and origin of some achondrite meteorite. Ph.D. dissertation, Univ. Oregon, Oregon, USA. 163 pp.

JONES J. (1989) Isotopic relationships among shergottites, the nakhlites and Chassigny. *Proc. Lunar Planet. Sci. Conf.* **19th**, 465–474.

JORON J. L., TREUIL M. AND RAIMBAUT L. (1997) Activation analyses as geochemical tool: Statement of its reliabilities for geochemical trace element studies. *J. Radioanal. Nucl. Chem.* **216**, 229–235.

KONG P., EBIHARA M. AND PALME H. (1999) Siderophile elements in martian meteorites and implications for core formation in Mars. *Geochim. Cosmochim. Acta* **63**, 1865–1875.

LAUL J. C. *ET AL.* (1986) Chemical systematics of the Shergotty meteorite and the composition of its parent body (Mars). *Geochim. Cosmochim. Acta* **50**, 909–926.

LOFGREN G., DONALDSON C. H., WILLIAMS R. J., MULLINS O., JR. AND USSELMAN T. M. (1974) Experimentally reproduced textures and mineral chemistry of Apollo 15 quartz-normative basalts. *Proc. Lunar Planet. Sci. Conf.* **5th**, 549–567.

LUNDBERG L. L., CROZAZ G., MCKAY G. A. AND ZINNER E. (1988) Rare earth element carriers in the Shergotty meteorite and implications for its chronology. *Geochim. Cosmochim. Acta* **52**, 2147–2163.

MA M. S., LAUL J. C. AND SCHMITT R. A. (1981) Complementary REE patterns in unique achondrites such as ALHA77005 and shergottites and in the Earth. *Proc. Lunar Planet. Sci. Conf.* **12th**, 1349–1358.

MA M. S., LAUL J. C., SMITH M. R. AND SCHMITT R. A. (1982) Chemistry of shergottites Elephant Moraine A79001 and Zagami (abstract). *Lunar Planet. Sci.* **13**, 451–452.

MARTI K., KIM J. S., THAKUR A. N., MCCOY T. J. AND KEIL K. (1995) Signatures of the martian atmosphere in glass of the Zagami meteorite. *Science* **267**, 1981–1984.

MCCOY T. J. *ET AL.* (1992) Zagami product of a two stage magmatic history. *Geochim. Cosmochim. Acta* **56**, 3571–3582.

MCCOY T. J., WADHWA M. AND KEIL K. (1999) New lithologies in the Zagami meteorite: Evidence for fractional crystallization of a single magma unit on Mars. *Geochim. Cosmochim. Acta* **63**, 1249–1262.

MCSWEEN H. Y., JR. (1994). What we have learned about Mars from SNC meteorites. *Meteoritics* **29**, 757–779.

MCSWEEN H. Y., JR., EISENHOUR D. D., TAYLOR L. A., WADHWA M. AND CROZAZ G. (1996) QUE 94201 shergottite: Crystallization of a martian basaltic magma. *Geochim. Cosmochim. Acta* **60**, 4563–4569.

MCSWEEN H. Y., JR., GROVE T. L., LENTZ R. C. F., DANN J. C., HOLZHEID A. H., RICIPUTI L. R. AND RYAN J. C. (2001) Geochemical evidence for magmatic water in within Mars from pyroxenes in the Shergotty meteorite. *Nature* **409**, 487–490.

MEYER C. (1998) *Mars Meteorite Compendium–1998*. Earth Science and Solar System Exploration Division, NASA Johnson Space Center, Houston, Texas, USA.

MIKOUCHI T., MIYAMOTO M. AND MCKAY G. A. (1998) Mineralogy of Antarctic basaltic shergottite Queen Alexandra Range 94201: Similarities to Elephant Moraine A79001 (lithology B) martian meteorite. *Meteorit. Planet. Sci.* **33**, 181–189.

MIKOUCHI T., MIYAMOTO M. AND MCKAY G. A. (1999) The role of undercooling in producing igneous zoning trends in pyroxenes and maskelynites among basaltic martian meteorites. *Earth Planet. Sci. Lett.* **173**, 235–256.

NEAL C. R., TAYLOR L. A., ELY J. C., JAIN J. C. AND NAZAROV M. A. (2001) Detailed geochemistry of new shergottite, Dhofar 019 (abstract). *Lunar Planet. Sci.* **32**, #1671, Lunar and Planetary Institute, Houston, Texas, USA (CD-ROM).

ROMANEK C. S., PERRY E. C., TREIMAN A. H., SOCKI R. A., JONES J. H. AND GIBSON E. K., JR. (1998) Oxygen isotopic record of silicate alteration in the Shergotty–Nakhla–Chassigny meteorite Lafayette. *Meteorit. Planet. Sci.* **33**, 775–783.

RUBIN A. E., WARREN P. H., GREENWOOD J. P., VERISH R. S., LESHIN L. A., HERVIG R. L., CLAYTON R. N. AND MAYEDA T. K. (2000) Los Angeles: The most differentiated basaltic martian meteorite. *Geology* **28**, 1011–1014.

SAUTTER V., BARRAT J. A., JAMBON A., JAVOY M., M. LORAND J. P., GILLET P., JORON J. L. AND LESOURD M. (2002) A new martian meteorite from Morocco: The nakhlite North West Africa 817. *Earth Planet. Sci. Lett.* **195**, 223–238.

SHARP T. G., EL GORESY A., WOPENKA B. AND CHEN M. (1999) A post-stishovite polymorph in the meteorite Shergotty: Implications for the impact events. *Science* **284**, 1511–1513.

SHIH C-Y., NYQUIST L. E., BOGARD D. D., MCKAY G. A., WOODEN J. L., BANSAL B. M. AND WIESMANN H. (1982) Chronology and petrogenesis of young achondrites, Shergotty, Zagami and ALHA77005: Late magmatism on a geologically active planet. *Geochim. Cosmochim. Acta* **46**, 2323–2344.

SMITH J. V. AND HERVIG R. L. (1979) Shergotty meteorite: Mineralogy, petrography and minor elements. *Meteoritics* **14**, 121–142.

SMITH M. R., LAUL J. C., MA M. S., HUSTON T., VERKOUTEREN R. M., LIPSCHUTZ M. E. AND SCHMITT R. A. (1984) Petrogenesis of the SNC meteorites: Implications for their origin from a large, dynamic planet, possibly Mars. *Proc. Lunar Planet. Sci. Conf.* **14th**, *J. Geophys. Res.* **89 (Suppl.)**, B612–B630.

STELZNER TH. *ET AL.* (1999) An interdisciplinary study of weathering effects in ordinary chondrites from the Acfer region, Algeria. *Meteorit. Planet. Sci.* **34**, 787–794.

STÖFFLER D., OSTERTAG R., JAMMES C., PFANNSCHMIDT G., SEN GUPTA P. R., SIMON S. B., PAPIKE J. J. AND BEAUCHAMP R. H. (1986) Shock metamorphism and petrography of the Shergotty achondrite. *Geochim. Cosmochim. Acta* **50**, 889–913.

STOLPER E. AND MCSWEEN H. Y., JR. (1979) Petrology and origin of the shergottite meteorites. *Geochim. Cosmochim. Acta* **43**, 1475–1498.

THOMAS K. L., ROMANEK C. S., MCKAY D. S., KELLER L. P. AND GIBSON E. K., JR. (1996) Microanalysis of unique fine-grained minerals in the martian meteorite ALH 84001 (abstract). *Lunar Planet. Sci.* **27**, 1327–1328.

TREIMAN A. H. (1985) Amphibole and hercynite spinel in Shergotty and Zagami: Magmatic water, depth of crystallization and metasomatism. *Meteoritics* **20**, 229–243.

TREIMAN A. H., MCKAY G. A., BOGARD D. D., MITTLEFEHLDT D. W., WANG M. S., KELLER L., LIPSCHUTZ M. E., LINDSTROM M. M. AND GARRISON D. H. (1994) Comparison of the LEW 88516 and ALHA77005 martian meteorites: Similar but distinct. *Meteoritics* **29**, 581–592.

TREIMAN A. H., GLEASON J. D. AND BOGARD D. D. (2000) The SNC meteorites are from Mars. *Planet. Space Sci.* **48**, 1213–1220.

WADHWA M., MCSWEEN H. Y., JR. AND CROZAZ G. (1994) Petrogenesis of shergottite meteorites inferred from minor and trace element microdistributions. *Geochim. Cosmochim. Acta* **58**, 4213–4229.

WADHWA M., CROZAZ G., TAYLOR L. A. AND MCSWEEN H. Y., JR. (1998) Martian basalt (shergottite) Queen Alexandra Range 94201 and lunar basalt 15555: A tale of two pyroxenes. *Meteorit. Planet. Sci.* **33**, 321–328.

WÄNKE H. AND DREIBUS G. (1988) Chemical composition and accretion history of terrestrial planets. *Phil. Trans. Royal Soc. London* **A325**, 545–557.

WARREN P. H. AND KALLEMEYN G. W. (1987) A trio of meteoritic dunites and new data for Shergotty (abstract). *Lunar Planet. Sci.* **18**, 1056–1057.

WASSON J. T. AND KALLEMEYN G. W. (1988) Composition of chondrites. *Phil. Trans. Royal Soc. London* **A325**, 535–544.

WARREN P. H. AND KALLEMEYN G. W. (1996) Siderophile trace elements in ALH 84001, other SNC meteorites and eucrites: Evidence of heterogeneity, possibly time linked, in the mantle of Mars. *Meteorit. Planet. Sci.* **31**, 97–105.

WARREN P. H., KALLEMEYN G. W. AND KYTE F. T. (1999) Origin of planetary cores: Evidence from highly siderophile elements in martian meteorites. *Geochim. Cosmochim. Acta* **63**, 2105–2122.

WEBER I., GRESHAKE A. AND BISCHOFF A. (2000) Low-cristobalite in the martian meteorite Zagami (abstract). *Lunar Planet. Sci.* **31**, #1342, Lunar and Planetary Institute, Houston, Texas, USA (CD-ROM).

ZIPFEL J., SHERER P., SPETTEL B., DREIBUS G. AND SCHULTZ L. (2000) Petrology and chemistry of the new shergottite Dar al Gani 476. *Meteorit. Planet. Sci.* **35**, 95–106.

Forward

Table of Contents